Emerging hubs in phantom perception connectomics

Anusha Mohan [a], Dirk De Ridder [b], Sven Vanneste [a,*]

[a]Lab for Clinical & Integrative Neuroscience, School of Behavioral and Brain Sciences, The University of Texas at Dallas, USA
[b]Department of Surgical Sciences, Section of Neurosurgery, Dunedin School of Medicine, University of Otago, Dunedin, New Zealand

ARTICLE INFO

ABSTRACT

Brain networks are small-world networks typically characterized by the presence of hubs, i.e. nodes that have significantly greater number of links in comparison to other nodes in the network. These hubs act as short cuts in the network and promote long-distance connectivity. Long-distance connections increase the efficiency of information transfer but also increase the cost of the network. Brain disorders are associated with an altered brain connectome which reflects either as a complete change in the network topology, as in, the replacement of hubs or as an alteration in the connectivity between the hubs while retaining network structure. The current study compares the network topology of binary and weighted networks in tinnitus patients and healthy controls by studying the hubs of the two networks in different oscillatory bands. The EEG of 311 tinnitus patients and 256 control subjects are recorded, pre-processed and source-localized using sLORETA. The hubs of the different binary and weighted networks are identified using different measures of network centrality. The results suggest that the tinnitus and control networks are distinct in all the frequency bands but substantially overlap in the gamma frequency band. The differences in network topology in the tinnitus and control groups in the delta, theta and the higher beta bands are driven by a change in hubs as well as network connectivity; in the alpha band by changes in hubs alone and in the gamma band by changes in network connectivity. Thus the brain seems to employ different frequency band-dependent adaptive mechanisms trying to compensate for auditory deafferentation.

© 2016 The Authors. Published by Elsevier Inc. This is an open access article under the CC BY-NC-ND license (http://creativecommons.org/licenses/by-nc-nd/4.0/).

1. Introduction

Brain networks analogous to protein (Maslov and Sneppen, 2002), computer, and social networks (Albert and Barabási, 2002; Strogatz, 2001) are described as small-world networks (Kaiser and Varier, 2011; Sporns and Zwi, 2004; Watts, 1999) that balance network cost with network efficiency (Achard and Bullmore, 2007; Bullmore and Sporns, 2012; Latora and Marchiori, 2003). The nodes of a small-world network are connected to other nodes through short and long-distance connections (Bassett and Bullmore, 2006; Bullmore and Sporns, 2009; Watts and Strogatz, 1998). A small fraction of the nodes, called hubs, defined as nodes with significantly greater number of links in comparison to other nodes in the network (Barabasi and Albert, 1999), are connected directly with one another promoting long-distance connectivity thus increasing the global efficiency of information transfer (Achard and Bullmore, 2007; van den Heuvel and Sporns, 2011) and are instrumental in defining the small-world topology of the network. Different kinds of hubs exist, some predominantly connecting locally (= provincial hub) within a

module and some having a large number of long range connections (= connector hub) connecting spatially distant modules (Bullmore and Sporns, 2012). Densely interconnected connector hubs are responsible for the integration of functional modules and form a core rich-club network (Bullmore and Sporns, 2012; van den Heuvel and Sporns, 2011; Zamora-López et al., 2010). Since they play a central role in information transfer, they incur high cost and are presented to be the most vulnerable centers for damage (Crossley et al., 2014; Kaiser et al., 2007; Stam, 2014). Deviation from small-world properties of functional networks has been documented in brain disorders such as Parkinson's (Olde Dubbelink et al., 2014), Alzheimer's (Stam et al., 2007, 2009), schizophrenia (Bassett et al., 2008; Fornito and Bullmore, 2015), dementia (Agosta et al., 2013), and traumatic brain injury (Stam, 2014).

Tinnitus is the perception of a continuous phantom sound that is commonly hypothesized to be caused due to sensory deafferentation (Jastreboff, 1990; Noreña and Farley, 2013). There is now converging evidence showing that, analogous to other brain disorders, tinnitus could also be the result of aberrant network connectivity (Lanting et al., 2014; Vanneste et al., 2011c). The current study thus attempts to investigate the differences in the functional network topology of a tinnitus and a healthy adult brain by observing the hubs of the network of the two groups in different oscillatory bands using graph theory. In order to do so we propose two possible hypotheses - (a) functional networks of the tinnitus and healthy brain share similar hubs but

* Corresponding author at: Lab for Clinical & Integrative Neuroscience, School of Behavioral & Brain Sciences, University of Texas at Dallas, W 1966 Inwood Rd, Dallas, TX 75235, USA.
  E-mail address: sven.vanneste@utdallas.edu (S. Vanneste).
  URL: http://www.lab-clint.org (S. Vanneste).

differ in the way they are connected and (b) functional networks of the tinnitus and healthy brain are fundamentally different networks involving different hubs with some regions overlapping with the normal functional module.

There is evidence from imaging and electrophysiological studies that tinnitus, analogous to other disorders such as neuropathic pain, major depression disorder, schizophrenia, and Alzheimer's disease shows changes in connectivity in some of the resting state networks such as the default mode network, dorsal attention network, auditory resting state network, salience network and the executive control network in healthy individuals (De Ridder et al., 2011, 2014b; Husain and Schmidt, 2014; Schlee et al., 2009). Resting-state fMRI studies show an increase in functional connectivity of the executive control network with the limbic regions (Schmidt et al., 2013) and auditory resting state network (Burton et al., 2012), limbic regions with resting state auditory network (Burton et al., 2012; Maudoux et al., 2012; Schmidt et al., 2013) and default mode network with the limbic (Burton et al., 2012) and auditory resting state network (Maudoux et al., 2012) in the tinnitus group. At the same time, a decreased connectivity was reported between the executive control network and the visual resting state network (Burton et al., 2012) in the tinnitus group. These findings allude to the idea that the tinnitus network could essentially consist of the same regions as a healthy control network but connected differently. Conceptually, this could be related to transformers or shape-shifters, which are fictional characters that can change their shape from a robot to that of a supercar by just changing the connections between different parts.

On the other hand, at the molecular level, it has been proposed that a disease network is formed by the disintegration of the normal functional network and a shift of core nodes within the same network (Barabási, 2007). Since several diseases share similar traits, it is suggested that some regions of the different disease networks overlap, but a specific disease has dedicated hubs that are different from the normal functional network (Barabási, 2007; Barabasi et al., 2011). There is also evidence from neuroimaging studies modeling damage to the normal brain connectome that show that although many neurodegenerative disorders affect the hubs of the normal connectome, different diseases result in having different central hubs (Crossley et al., 2014). Tinnitus, is a multi-symptom disorder where the different characteristics of tinnitus such as the loudness, pitch, distress, type and laterality are proposed to be the result of different functional subnetworks working in tandem (De Ridder et al., 2014b) towards bringing these different characteristics of tinnitus to consciousness by linking to consciousness supporting networks (De Ridder et al., 2014b; Dehaene et al., 2006; Schlee et al., 2009). The tinnitus loudness network has been proposed to consist of the auditory cortices and the parahippocampal areas (De Ridder et al., 2013; Husain and Schmidt, 2014), the distress network consists of the precuneus, insula, pregenual, subgenual and dorsal anterior cingulate cortex (Husain and Schmidt, 2014; Mayberg et al., 2005; Vanneste et al., 2010a; Weisz et al., 2005), the type of the tinnitus encoded by the frontopolar cortex, posterior cingulate cortex and the parahippocampus (De Ridder et al., 2014b) and the laterality of the tinnitus encoded by the gamma band activity in the contralateral parahippocampus (Vanneste et al., 2011b). Schlee et al. (2007) also showed using magnetoencephalography that the tinnitus distress was significantly correlated with the connectivity strength between pairs of regions selected in the temporal, prefrontal and parietal regions (Schlee et al., 2007). They allude to the possibility of a dedicated tinnitus distress network possibly consisting of the right parietal cortex, temporal regions and the anterior cingulum. In addition, tinnitus is viewed as the perception of a sound which is being constantly re-called from memory (De Ridder et al., 2006; Laureano et al., 2014) with the help of an active fronto-temporal memory retrieval network (Vanneste et al., 2011c) thus, alluding to tinnitus having a fundamentally different network structure compared to a control network.

In order to answer this research question, the most important nodes of both the binary and weighted functional networks in tinnitus patients and healthy controls are compared by looking at different centrality measures. A large overlap among the hubs of the two groups would allude to the transformer model of network organization and the appearance of distinct hubs would allude to a fundamentally different network topology in tinnitus and controls. The results of the current study are important in understanding the network structure of the tinnitus network and confirms the idea of several researchers about the existence of a wide spread network in tinnitus (De Ridder et al., 2014b; Schlee et al., 2007, 2009). Moreover, it could also provide a relationship between the network connectivity measures and effectiveness of a treatment procedure, especially given the volume of research now being presented in tinnitus treatment techniques. Such a study was presented by Hartmann and colleagues, where they evaluated the effectiveness of neurofeedback, rTMS and sham in increasing the alpha power thus enhancing the inhibitory mechanism (Hartmann et al., 2014). Moving forward, the results of the current study could provide more sophisticated techniques in addition to the one provided in the study mentioned above and help us evaluate different treatment measures, which are now gaining traction in the field of neuromodulation.

2. Materials and methods

2.1. Patients with an auditory phantom percept

The patient sample consisted of 311 patients ($M = 50.24$ years; $SD = 14.32$; 210 males and 101 females) with continuous tinnitus. If the onset of the tinnitus was reported to be a year or more, the patient's condition was considered chronic. The homogeneity of the sample was increased by excluding individuals with pulsatile tinnitus, Ménière disease, otosclerosis, chronic headache, neurological disorders such as brain tumors, and individuals being treated for mental disorders from the study. Patients reported the perceived location of their tinnitus (the left ear, in both ears, and centralized in the middle of the head (bilateral), the right ear) including the type of tinnitus (pure tone-like tinnitus or noise-like tinnitus). Pure tone audiometric thresholds at .125 kHz, .25 kHz, .5 kHz, 1 kHz, 2 kHz, 3 kHz, 4 kHz, 6 kHz and 8 kHz were obtained using the British Society of Audiology procedures (Audiology, 2008). The pitch and loudness of the tinnitus were measured by performing a simple analysis on the ear contralateral to the tinnitus ear in patients with unilateral tinnitus and contralateral to the worst tinnitus ear in patients with bilateral tinnitus. A 1 kHz pure tone was presented contralateral to the (worst) tinnitus ear at 10 dB above the patient's hearing threshold in that ear. The frequency of the tone was adjusted until the pitch of the tone matched the perceived pitch of the patient's tinnitus. The intensity of this tone was then adjusted in a similar way until it corresponded to the perceived loudness of the patient's tinnitus. The tinnitus loudness (dB SL) was computed by subtracting the audiometric threshold from the absolute tinnitus loudness (dB HL) at that frequency (Meeus et al., 2009, 2011). See Table 1 for an overview of the tinnitus characteristics. This study was approved by the local ethical committee (Antwerp University Hospital) and was in accordance with the declaration of Helsinki.

2.2. Healthy control group

A healthy control group (N = 256; $M = 49.514$ years; $SD = 14.82$; 154 males and 102 females) was included in the study. None of these subjects reported to suffer from tinnitus. Psychiatric or neurological illness, history of psychiatric or drug/alcohol abuse, history of head injury (with loss of consciousness) or seizures, headache, or physical disability were the exclusion criteria for the study. No hearing assessment was performed for these healthy controls.

Table 1
Characteristics of tinnitus patients.

Ear	
Unilateral	114
Bilateral	197
Tone	
Pure tone	118
Noise like	193
TQ	
Mean	39.37
SD	17.59
Tinnitus frequency (Hz)	
Mean	5143
SD	3183
Hearing loss at the tinnitus frequency (dB SL)	
Mean	7.85
SD	8.78

2.3. Data collection

The data was collected under approval of IRB UZA OGA85. All patients gave an informed consent. Continuous resting state Electroencephalograph (EEG) data was recorded in both subject groups in an eyes closed condition for five minutes (sampling rate = 500 Hz, band passed 0.15–200 Hz). The room where the recordings were obtained was fully lit with the participant sitting upright on a comfortable chair. The EEG was sampled using Mitsar-201 amplifiers (NovaTech http://www.novatecheeg.com/). EEG was recorded using 19 electrodes placed according to the standard 10–20 International placement (Fp1, Fp2, F7, F3, Fz, F4, F8, T7, C3, Cz, C4, T8, P7, P3, Pz, P4, P8, O1, O2) referenced to digitally linked ears. Impedances were maintained below 5 kΩ. The data was analyzed off-line. This included re-sampling at 128 Hz and band-pass filtering in the 2–44 Hz range. The data was subsequently transposed into Eureka! software (Congedo, 2002), for plotting and manual rejection of artifacts. All episodic artifacts including eye blinks, eye movements, teeth clenching, body movement, or ECG artifact were removed from the EEG. Average Fourier cross-spectral matrices were computed for frequency bands delta (2–3.5 Hz), theta (4–7.5 Hz), alpha1 (8–10 Hz), alpha2 (10–12 Hz), beta1 (13–18 Hz), beta2 (18.5–21 Hz), beta3 (21.5–30 Hz) and gamma (30.5–44 Hz). These frequency bands are based on previous research in tinnitus (Song et al., 2013a,b; Vanneste and De Ridder, 2011; Vanneste et al., 2010b, 2011a).

2.4. Source localization

Standardized low-resolution brain electromagnetic tomography (sLORETA; Pascual-Marqui, 2002) was used as the primary technique to estimate the intracerebral electrical sources. As a standard procedure, a common average reference transformation (Pascual-Marqui, 2002) was done before applying the sLORETA algorithm. sLORETA computes neuronal activity in current density (A/m^2) without assuming a predefined number of active sources. The solution space used in this study and associated lead field matrix are those implemented in the LORETA-Key software (freely available at http://www.uzh.ch/keyinst/loreta.htm). This software implements the lead field and the revisited realistic electrode coordinates by applying the boundary element method on the MNI-152 (Montreal neurological institute, Canada) template. The sLORETA-key anatomical template divides and labels the neocortical (including hippocampus and anterior cingulate cortex) MNI-152 volume into 6239 voxels each of size 5 mm³, based on the probabilities returned by the Daemon Atlas.

2.5. Lagged phase coherence

Lagged phase coherence between two sources can be interpreted as the amount of cross-talk between different regions contributing to the source activity (Congedo et al., 2010). Since the two sources oscillate coherently with a lag in phase, the coherence can be interpreted as information sharing by axonal transmission (Congedo et al., 2010). More precisely, the discrete Fourier transform decomposes the signal in a finite series of cosine and sine waves (in-phase and out-of-phase carrier waves, that form the real and imaginary part of the Fourier decomposition). The lag of the cosine waves in relation to their sine counterparts is inversely proportional to the frequency and contributes to a quarter of the period; for example, the period of a sinusoidal wave at 10 Hz is 100 ms. The sine is shifted by a quarter of a cycle (25 ms) with the respect to the cosine. Then the lagged phase coherence at 10 Hz indicates coherent oscillations with a 25 ms delay, while at 20 Hz the delay is 12.5 ms, and so on. A cross-spectral coherence of the two time series is computed and the lagged coherence is obtained by dividing the imaginary part of the cross-spectral coherence by the whole root of 1 minus the square of the real part of the cross spectral coherence. The formula and a detailed explanation is provided in (Pascual-Marqui et al., 2011). The threshold of significance for a given lagged phase coherence value according to asymptotic results and the definition of lagged phase coherence is described by Pascual-Marqui et al. (2011). This analysis was corrected for the amount of pair wise comparisons using a Bonferroni correction. The time-series of current density was extracted for all regions of interest using sLORETA for all the frequency bands delta (2–3.5 Hz), theta (4–7.5 Hz), alpha1 (8–10 Hz), alpha2 (10–12 Hz), beta1 (13–18 Hz), beta2 (18.5–21 Hz), beta3 (21.5–30 Hz) and gamma (30.5–44 Hz). The regions of interest consist of the 84 Brodmann areas and the values of the lagged phase coherence between each pair-wise combination of Brodmann area signifies the functional connectivity strength between them. Fig. 1 shows locations of the 84 Brodmann areas and the explanation to the abbreviations to the names of the regions is given in Table 2.

2.6. Weighted and adjacency matrices

A threshold is introduced in order to observe the consistency in the occurrence of hubs (Achard and Bullmore, 2007; Bassett et al., 2008; Stam et al., 2007). One potential problem of introducing thresholds is that one has to control for the number of edges in the tinnitus and control networks that could vary depending on the connection weights (Langer et al., 2013). Thus, the current study controls for the number of edges and also employs a maximum spanning tree analysis which is a data-driven process that controls for both the number of edges and number of nodes in the final tree (Stam et al., 2014). The network of the 84 Brodmann areas and the corresponding lagged phase coherence between all pair-wise combinations of Brodmann areas represent the fully connected, undirected network with 84 nodes and 3486 unidirectional edges.

A threshold of .005 was introduced on the connectivity strength uniformly across all the eight frequency bands so that the resulting network retained the 84 nodes. However, the number of edges in each of the frequency bands was different and was also different among tinnitus and control groups. The weighted networks at a threshold of .005 were converted to binary matrices by coding the presence of a connection between two Brodmann areas as one and the absence of a connection as zero. In order to compare fully connected binary networks with the same number of edges, different values of thresholds were introduced at the different frequency bands ensuring that the tinnitus and control groups had equal number of edges and were still fully connected. The connection weights were then coded one or zero depending on the presence or absence of a connection.

2.7. Maximum spanning tree

Introducing thresholds cannot accurately create networks with equal number of nodes and edges. In order to compare sub-networks with the same number of edges and nodes, a maximum spanning tree
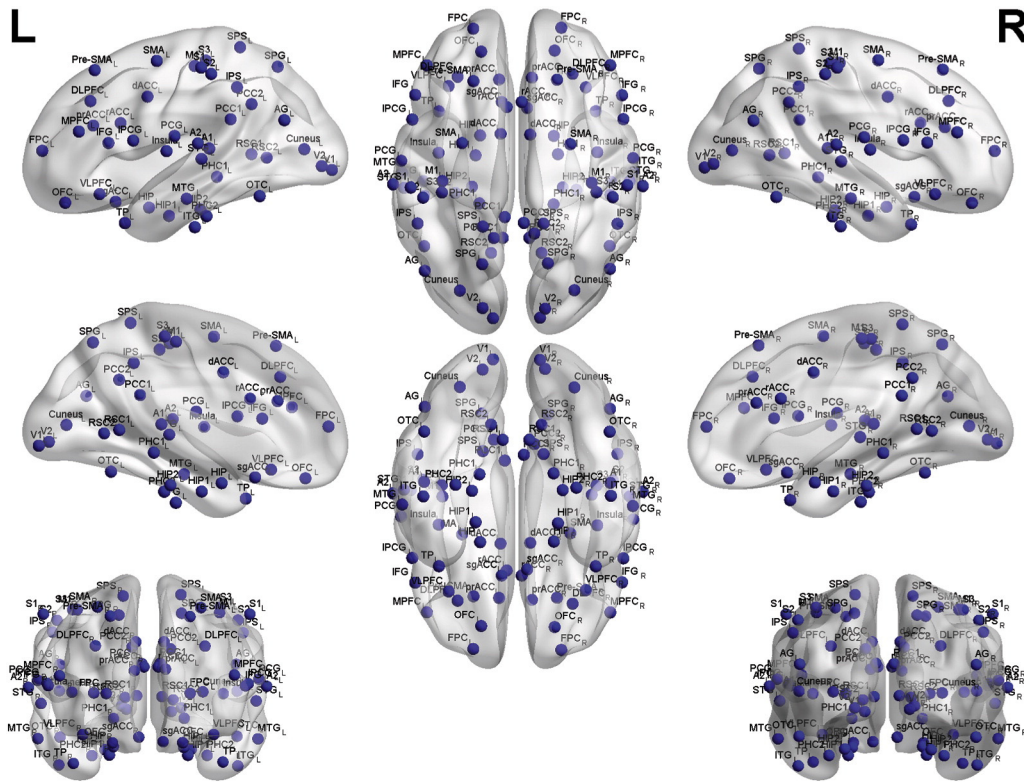
Fig. 1. All the Brodmann areas included in this study.

can be drawn using a data-driven algorithm. The maximum spanning tree is a subnetwork which has N nodes and N-1 edges. The maximum spanning tree is derived from the fully-connected weighted network using Kruskal's algorithm (Kruskal, 1956; Wang et al., 2010). All the possible unidirectional edges of the network are arranged in descending order of their weights or connectivity strengths. The edges are then sequentially added to the maximum spanning tree and when the algorithm encounters an edge that would create a loop with any of the remaining edges, that edge is not added in the tree. This continues until all the edges are scanned through. Hubs in a maximum spanning tree are calculated based on the degree and betweenness centrality of the nodes as explained below. In the current study, the maximum spanning tree in each of the frequency bands and two groups contain 84 nodes and 83 edges.

The hubs of the binary and weighted networks in both groups at each frequency band were identified using the degree, node strength, betweenness centrality, eigenvector centrality, and closeness centrality of each node. Nodes with one or more nodal measures bearing a value greater than one standard deviation from the mean value of the measure were considered the hubs of the network (Bassett et al., 2008; van den Heuvel and Sporns, 2011). These measures were calculated using the Brain Connectivity Toolbox developed by Rubinov and Sporns (2010).

2.8. Degree

Degree is the number of nodes connected to each node in the network (Rubinov and Sporns, 2010).

2.9. Betweenness centrality

The betweennness centrality reflects the centrality of a node in a network, assuming information transfer follows the shortest path. Therefore, a node with a high betweennness centrality has a large influence on information transmission in the network.

The betweenness centrality of a node is the fraction of the total number of shortest paths that pass through it. It is calculated by examining all the paths passing through a node and summing the number of shortest paths that pass through it, relative to the total number of nodes (Rubinov and Sporns, 2010). The connection weights are converted to connection-length matrices by taking the mathematical inverse of the weighted matrix. The shortest path between any two nodes in the network is then calculated using Dijkstra's algorithm (Dijkstra, 1959). Both the shortest distance between pairs of nodes and the betweenness centrality of each node is determined by appropriate functions from the Brain Connectivity Toolbox (Rubinov and Sporns, 2010).

2.10. Eigenvector centrality

The eigenvector centrality is another measure of the influence a node has on the network. It assumes that connections to high-scoring nodes contribute more to the score of the particular node than equal connections to low-scoring nodes. The eigenvector centrality of a node expresses the capability of the node to be able to connect with other nodes with a high eigenvalue. The eigenvector of the functional connectivity matrix with the largest eigenvalues were considered the measure of eigenvector centrality (Rubinov and Sporns, 2010).

2.11. Closeness centrality

The closeness centrality of a node is a measure of how close a node is from every other node in the network. The closeness centrality was calculated as the inverse of the mean of the shortest paths from one node to every other node normalized by the total number of nodes in the network (Rubinov and Sporns, 2010).

2.12. Common hubs

Once the hubs were identified using the different techniques, those hubs that were commonly identified using two or more techniques

Table 2
All the Brodmann areas included in the study.

Brodmann areas	Abbreviation	Name of the Brodmann area
BA01	S1	Primary somatosensory cortex
BA02	S2	Secondary somatosensory cortex
BA03	S3	Tertiary somatosensory cortex
BA04	M1	Primary motor cortex
BA05	SPS	Superior parietal sulcus
BA06	SMA	Supplementary motor area
BA07	SPG	Superior parietal gyrus
BA08	Pre-SMA	Pre-supplementary motor area
BA09	DLPFC	Dorsolateral prefrontal cortex
BA10	FPC	Fronto-parietal cortex
BA11	OFC	Orbital frontal cortex
BA13	Insula	Insula
BA17	V1	Primary visual cortex
BA18	V2	Secondary visual cortex
BA19	Cuneus	Cuneus
BA20	ITG	Inferior temporal gyrus
BA21	MTG	Medial temporal gyrus
BA22	STG	Superior temporal gyrus
BA23	PCC1	Posterior cingulate cortex1
BA24	dACC	Dorsal anterior cingulate cortex
BA25	sgACC	Subgeneual anterior cingulate cortex
BA27	PHC1	Parahippocampal gyrus1
BA28	HIP1	Hippocampal area1
BA29	RSC1	Retrosplenial cortex1
BA30	RSC2	Retrosplenial cortex2
BA31	PCC2	Posterior cingulate cortex2
BA32	prACC	Pregeneual anterior cingulate cortex
BA33	rACC	Rostral anterior cingulate cortex
BA34	HIP	Hippocampus
BA35	HIP2	Hippocampal area2
BA36	PHC2	Parahippocampal gyrus2
BA37	OTC	Occipital–temporal cortex
BA38	TP	Temporal pole
BA39	AG	Angular gyrus
BA40	IPS	Intra-parietal sulcus
BA41	A1	Primary auditory cortex
BA42	A2	Secondary auditory cortex
BA43	PCG	Postcentral gyrus
BA44	OPCG	Opercular part of inferior frontal gyrus
BA45	IFG	Inferior frontal gyrus
BA46	MPFC	Medial prefrontal cortex
BA47	VLPFC	Ventero-lateral prefrontal cortex

across the different frequency bands were labeled separately and compared between tinnitus and control groups.

2.13. Statistical analysis

Two tailed simple contrasts at a significance level of $p = .05$ were used to compare the different network centrality measures derived using the different techniques between the two groups and across the eight frequency bands.

3. Results

3.1. Fully-connected weighted network

1. Betweenness centrality

We do not observe a significant main effect of Groups for the average betweenness centrality which implies that the mean betweenness centrality of the tinnitus group is not significantly different from that of the control group ($F = .08$, $p = .781$). There is no change observed with the mean value of betweenness centrality with frequency ($F = 1.04$, $p = .393$) (Fig. 2a).

2. Node strength

We observe a significant main effect of groups for the average node strength ($F = 15.10$, $p < .001$) that is significantly moderated by the different frequency bands ($F = 34.50$, $p < .001$). Simple contrasts on node strength revealed that the mean strength of a node in the tinnitus network is significantly different from the control in delta ($F = 124.62$, $p < .001$), theta ($F = 863.65$, $p < .001$), alpha2 ($F = 12.83$, $p < 0.001$), beta1 ($F = 47.80$, $p < .001$), beta2 ($F = 36.36$, $p < .001$) and beta3 ($F = 110.97$, $p < .001$) frequency bands. No significant effect could be obtained for the alpha1 ($F = 2.51$, $p < .115$) and gamma ($F = 1.15$, $p < .285$) frequency bands (Fig. 2b).

3. Eigenvector centrality

No significant main effect of groups was observed for the eigenvector centrality ($F = .01$, $p = .919$). Hence, the mean eigenvector centrality of the tinnitus network is not significantly different from that of the control. This average value of the eigenvector centrality was not significantly moderated by the different frequency bands ($F = 2.22$, $p = .088$) (Fig. 2c).

4. Closeness centrality

The mean closeness centrality of the tinnitus group was observed to be significantly different from that of the control group ($F = 68.75$, $p < .001$). This effect was significantly moderated across the different frequency bands ($F = 133.83$, $p < .001$). A simple contrast on closeness centrality revealed that the average closeness centrality of the tinnitus network is significantly different from that of the controls in delta ($F = 280.30$, $p < .001$), theta ($F = 2593.19$, $p < .001$), alpha1 ($F = 18.26$, $p < .001$), alpha2 ($F = 92.80$, $p < .001$), beta1 ($F = 190.50$, $p < .001$), beta2 ($F = 99.55$, $p < .001$), beta3 ($F = 413.83$, $p < .001$) and gamma ($F = 13.77$, $p < .001$) frequency bands (Fig. 2d). The hubs calculated from the fully-connected weighted network in the eight frequency bands are shown in Fig. 3a–h. A table consisting of the hubs in the fully connected weighted network is provided in Supplementary Table 1.

3.2. Binary network with equal edges in tinnitus and controls

1. Betweenness centrality

We observe no significant main effect of groups for the average values of betweenness centrality ($F = .79$, $p = .376$) nor is it significantly moderated by frequency bands ($F = 1.30$, $p = .257$) (Fig. 2e).

2. Node strength

We observe no main effect of group on the average values of node strength ($F = 2.24$, $p = .136$). However, the average value of the node strength in the tinnitus and control groups is significantly moderated by the frequency bands ($F = 5.73$, $p < .001$). Simple contrasts for node strength reveal that a significant difference in the average node strength between tinnitus and control is observed only in the theta ($F = 57.69$, $p < .001$) frequency band and no significant difference was observed at the delta ($F = .003$, $p = .957$), alpha1 ($F = .004$, $p = .948$), alpha2 ($F = .046$, $p = .831$), beta1 ($F = .00$, $p = .991$), beta2 ($F = .02$, $p = .903$), beta3 ($F = 00$, $p = .983$) and gamma ($F = .00$, $p = .984$) frequency bands (Fig. 2f).

3. Eigenvector centrality

We observe no significant effect of groups on the average eigenvector centrality ($F = .01$, $p = .916$). Moreover, the average value of eigenvector centrality is not significantly moderated by frequency bands ($F = .33$, $p = .861$) (Fig. 2g).

4. Closeness centrality

We find a significant difference in the average closeness centrality between tinnitus and controls ($F = 14.28$, $p < .001$). The effects of the
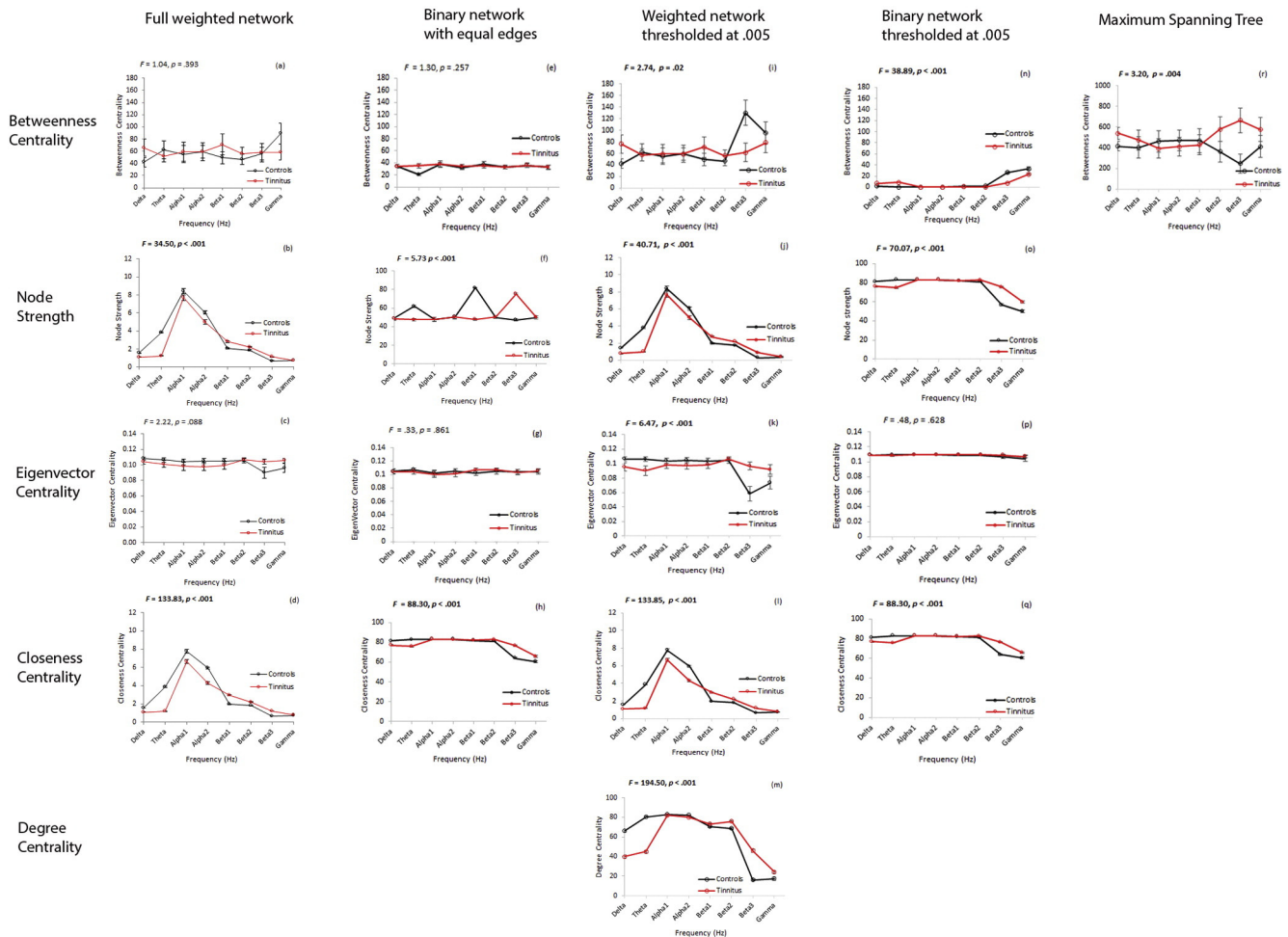
Fig. 2. Network centrality measures from the different analysis techniques. (a)–(d) Full weighted network, (e)–(h) binary network with equal edges, (i)–(m) weighted network thresholded at .005, (n)–(q) binary network thresholded at .005, (r) maximum spanning tree. Average measures of betweenness centrality, node strength, eigenvector centrality, closeness centrality and degree centrality are calculated on the different networks in control (black) and tinnitus (red) groups in the eight frequency bands. The bars represent the standard error about the mean of the data. (For interpretation of the references to color in this figure legend, the reader is referred to the web version of this article.)

average closeness centrality is significantly moderated by the different frequency bands ($F = 88.30, p < .001$). Simple contrasts for the average closeness centrality across the different frequency bands reveal a significant difference between the average closeness centrality between tinnitus and controls in delta ($F = 42.53, p < .001$), theta ($F = 130.67, p < .001$), beta2 ($F = 25.68, p < .001$), beta3 ($F = 167.47, p < .001$) and gamma ($F = 19.13, p < .001$) frequency bands and no significant difference in alpha1 ($F = .00$), alpha2 ($F = .93, p = .336$) and beta1 ($F = .56, p = .454$) bands (Fig. 2h). The hubs calculated from the binary network with equal edges in the tinnitus and control group in the eight frequency bands are shown in Fig. 4a–h. A table consisting of the hubs in the binary network with equal edges is provided in Supplementary Table 2.

3.3. Weighted connectivity matrix thresholded at .005

1. Betweenness centrality

We observe no significant effect of groups for betweenness centrality ($F = .06, p = .806$) but observe that the average values of betweenness centrality is significantly moderated by frequency bands ($F = 2.74, p = .019$). Simple contrasts for betweenness centrality over the eight frequency bands reveal that no significant differences were observed between the average values in the tinnitus and controls groups in

delta ($F = 3.51, p = .063$), theta ($F = .06, p = .804$), alpha1 ($F = .04, p = .851$), alpha2 ($F = .00, p = .998$), beta1 ($F = 1.14, p = .287$), beta2 ($F = .54, p = .463$), and gamma ($F = .46, p = .499$) frequency bands except the beta3 ($F = 6.58, p = .011$) frequency band (Fig. 2i).

2. Node strength

We observe a significant effect of groups for the average node strength ($F = 17.03, p < .001$) and that this effect is significantly moderated by frequency ($F = 40.71, p < .001$). Simple contrasts for node strength reveal that a significant difference in the average values between tinnitus and controls was observed in delta ($F = 147.13, p < .001$), theta ($F = 947.06, p < .001$), alpha2 ($F = 13.19, p < .001$), beta1 ($F = 46.69, p < .001$), beta2 ($F = 37.64, p < .001$) and beta3 ($F = 114.85, p < .001$ frequency bands and no significant difference was observed in alpha1 ($F = 2.55, p = .112$)) and gamma ($F = .85, p = .357$) frequency bands (Fig. 2j).

3. Eigenvector centrality

We observe no significant effect of groups for the average measures of eigenvector centrality ($F = .20, p = .660$). The average eigenvector centrality is, however, significantly moderated by the frequency bands ($F = 6.47, p < .001$). Simple contrasts for eigenvector centrality reveal
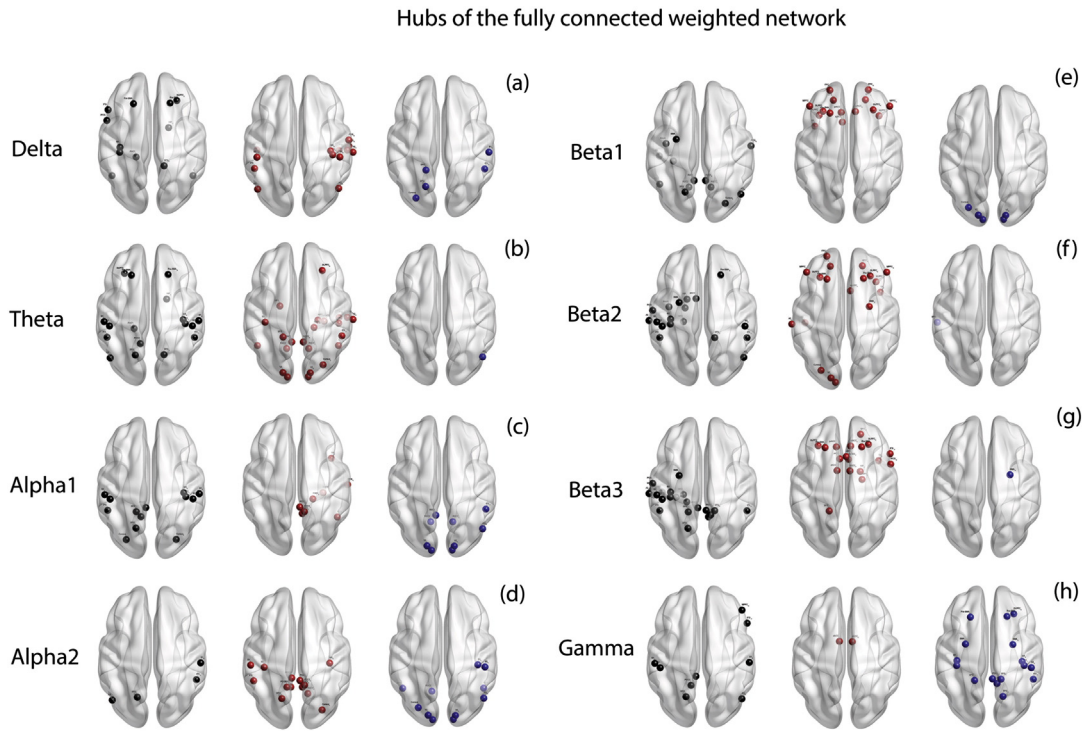
Hubs of the fully connected weighted network

Fig. 3. Hubs of the fully connected weighted network. (a)–(h) represent the hubs identified in the fully connected weighted network in *left*: controls (black dots) only, *middle*: tinnitus (red dots) only and *right*: those hubs that are common to both tinnitus and control groups (blue dots) in (a) delta, (b) theta, (c) alpha1, (d) alpha2, (e) beta1, (f) beta2, (g) beta3 and (h) gamma frequency bands. (For interpretation of the references to color in this figure legend, the reader is referred to the web version of this article.)

that a significant difference in the average values was observed between tinnitus and controls in beta3 ($F = 11.16$, $p = .001$) and theta ($F = 4.63$, $p = .033$) and no difference was observed at delta ($F = 3.04$, $p = .083$), alpha1 ($F = .81$, $p = .370$), alpha2 ($F = 1.33$, $p = .250$), beta1 ($F = .56$, $p = .457$), beta2 ($F = .24$, $p = .624$) and gamma ($F = 2.83$, $p = .094$) frequency bands (Fig. 2k).
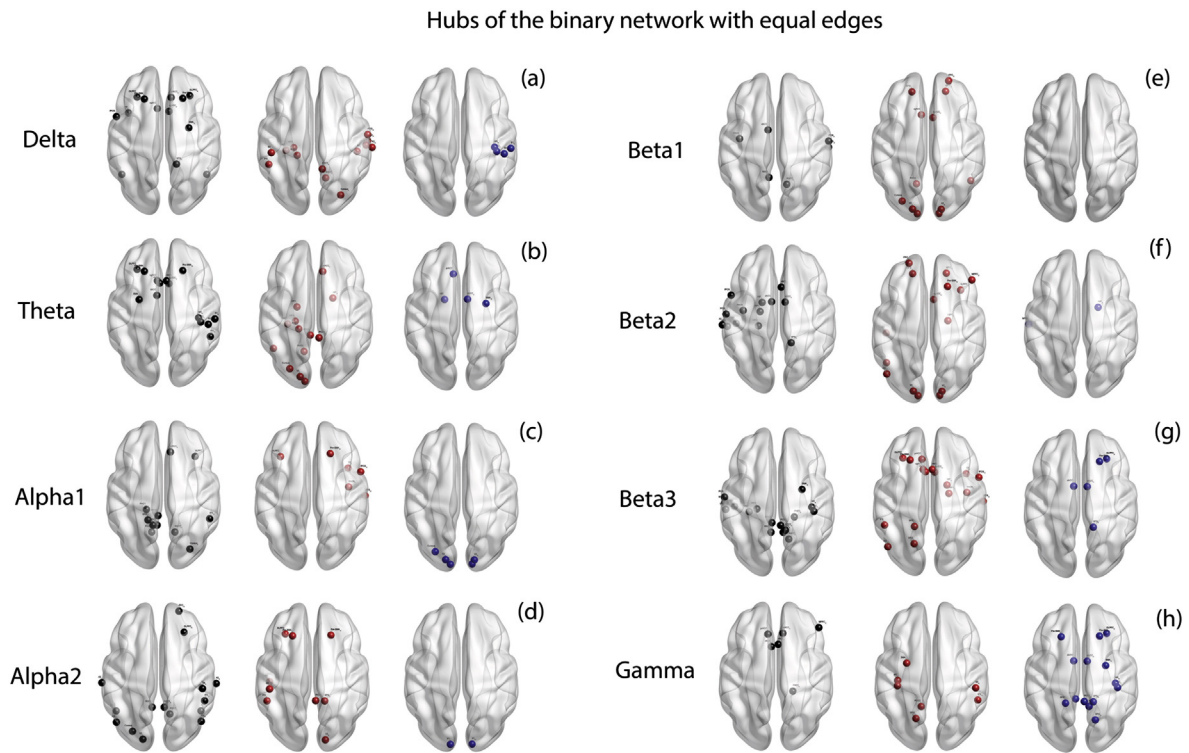
Hubs of the binary network with equal edges

Fig. 4. Hubs of the binary network with equal edges. (a)–(h) represent the hubs identified in the binary network with equal edges in *left*: controls (black dots) only, *middle*: tinnitus (red dots) only and *right*: those hubs that are common to both tinnitus and control groups (blue dots) in (a) delta, (b) theta, (c) alpha1, (d) alpha2, (e) beta1, (f) beta2, (g) beta3 and (h) gamma frequency bands. (For interpretation of the references to color in this figure legend, the reader is referred to the web version of this article.)

4. Closeness centrality

We observe a significant effect of groups for the average values of closeness centrality ($F = 68.70$, $p < .001$), indicating that the average values of closeness centrality are significantly different between tinnitus and controls. The group effect is also significantly moderated by frequency bands ($F = 133.85$, $p < .001$). Simple contrasts for closeness centrality revealed that the average values were significantly different in the tinnitus and control groups in delta ($F = 280.29$, $p < .001$), theta ($F = 2593.19$, $p < .001$), alpha1 ($F = 18.26$, $p < .001$), alpha2 ($F = 92.80$, $p < .001$), beta1 ($F = 190.50$, $p < .001$), beta2 ($F = 99.55$, $p < .001$), beta3 ($F = 413.97$, $p < .001$) and gamma ($F = 13.94$, $p < .001$) frequency bands (Fig. 2i).

5. Degree centrality

We observe a significant main effect of groups for the average measure of degree centrality ($F = 10.18$, $p < .001$). The group effect is significantly moderated by the frequency bands ($F = 194.50$, $p < .001$). Simple contrasts reveal that a significant difference in the average values of degree centrality between tinnitus and controls is observed at delta ($F = 160.57$, $p < .001$), theta ($F = 575.64$, $p < .001$), alpha1 ($F = 27.57$, $p < .001$), alpha2 ($F = 30.59$, $p < .001$), beta1 ($F = 4.01$, $p = .047$), beta2 ($F = 31.77$, $p < .001$), beta3 ($F = 192.28$, $p < .001$) and gamma ($F = 11.12$, $p = .001$) frequency bands (Fig. 2m). The hubs calculated from the weighted network thresholded at .005 in the two groups in the eight frequency bands are indicated in Fig. 5a–h. A table consisting of the hubs in the thresholded weighted network is provided in Supplementary Table 3.

3.4. Binary connectivity matrix thresholded at .005

1. Betweenness centrality

We observe a significant main effect of groups for the average values of betweenness centrality ($F = 15.05$, $p < .001$) that is significantly moderated by the different frequency bands ($F = 38.89$, $p < .001$). Simple contrasts across the eight frequency bands reveal that the average betweenness centrality of tinnitus is significantly different from the controls only at the delta ($F = 317.18$, $p < .001$), theta ($F = 476.95$, $p < .001$), alpha2 ($F = 681.48$, $p < .001$), beta1 ($F = 42.80$, $p < .001$), beta2 ($F = 866.50$, $p < .001$), beta3 ($F = 93.12$, $p < .001$) and gamma ($F = 8.35$, $p = .004$) frequency bands and not significantly different for the alpha1 ($F = .00$) frequency band (Fig. 2n).

2. Node strength

We observe a significant effect of groups for the average values of node strength ($F = 22.52$, $p < .001$) that is significantly moderated by the different frequency bands ($F = 70.07$, $p < .001$). Simple contrasts for node strength reveal that a significant difference in the average node strength between tinnitus and control is observed in the delta ($F = 39.00$, $p < .001$), theta ($F = 99.46$, $p < .001$), beta2 ($F = 23.37$, $p < .001$), beta3 ($F = 144.51$, $p < .001$) and gamma ($F = 19.98$, $p < .001$) frequency bands and no significant difference was observed at the alpha1 ($F = .00$), alpha2 ($F = .93$, $p = .337$) and beta1 ($F = .65$, $p = .423$) frequency bands (Fig. 2o).

3. Eigenvector centrality

We observe no significant effect of groups for the average values of eigenvector centrality between tinnitus and control groups ($F = .45$,
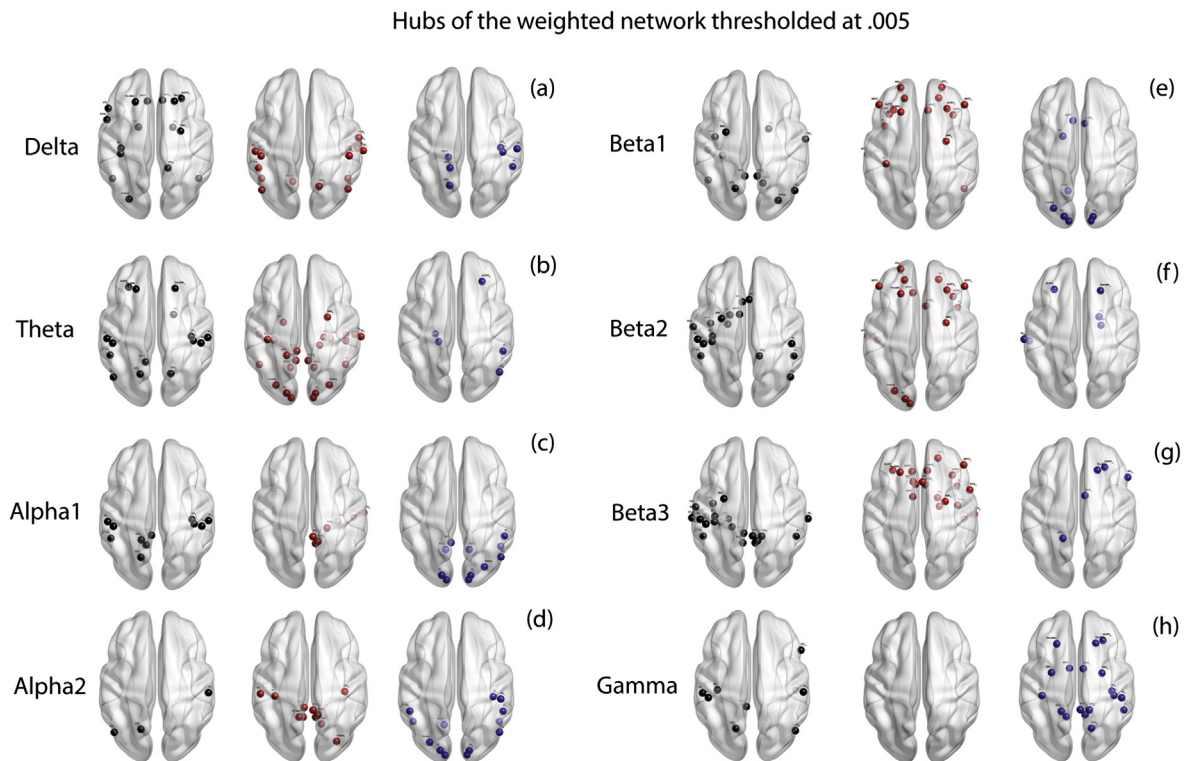
Hubs of the weighted network thresholded at .005

Fig. 5. Hubs of the weighted network thresholded at .005. (a)–(h) represent the hubs identified in the weighted network thresholded at .005 in *left*: controls (black dots) only, *middle*: tinnitus (red dots) only and *right*: those hubs that are common to both tinnitus and control groups (blue dots) in (a) delta, (b) theta, (c) alpha1, (d) alpha2, (e) beta1, (f) beta2, (g) beta3 and (h) gamma frequency bands. (For interpretation of the references to color in this figure legend, the reader is referred to the web version of this article.)

$p = .505$) nor are these values significantly moderated by the frequency bands ($F = .48$, $p = .628$) (Fig. 2p).

4. Closeness centrality

We observe a significant effect of groups for the average values of closeness centrality ($F = 14.28$, $p < .001$) which is significantly moderated by the eight frequency bands ($F = 88.30$, $p < .001$). Simple contrasts for closeness centrality across the different frequency bands reveal a significant difference between the average closeness centrality between tinnitus and controls in delta ($F = 42.53$, $p < .001$), theta ($F = 130.67$, $p < .001$), beta2 ($F = 25.68$, $p < .001$), beta3 ($F = 167.47$, $p < .001$) and gamma ($F = 19.13$, $p < .001$) frequency bands and no significant difference in alpha1 ($F = .00$), alpha2 ($F = .93$, $p = .336$) and beta1 ($F = .56$, $p = .454$) bands (Fig. 2q). The hubs calculated from the binary networks thresholded at .005 from the full network of the two groups in the eight frequency bands are shown in Fig. 6a–h. A table consisting of the hubs in the thresholded binary is provided in Supplementary Table 4.

3.5. Maximum spanning tree

1. Betweenness centrality

We observe no significant main effect of groups for the average betweenness centrality ($F = .76$, $p = .383$) implying that no significant difference is observed between the average values of betweenness centrality between tinnitus and controls. These values are however significantly moderated by the frequency bands ($F = 3.20$, $p = .004$) Simple contrasts reveal that the average betweenness centrality of the tree is significantly different between the tinnitus and controls only at beta3 ($F = 7.69$, $p = .006$) frequency band and is not significantly different at delta ($F = .77$, $p = .383$), theta ($F = .27$, $p = .603$), alpha1 ($F = .26$, $p = .612$), alpha2 ($F = .21$, $p = .647$), beta1 ($F = .07$, $p = .788$), beta2 ($F = 1.92$, $p = .168$) and gamma ($F = 1.10$, $p = .297$) frequency

bands (Fig. 2r). The hubs of the maximum spanning tree of the networks in the two groups and eight frequency bands are shown in Fig. 7a–h. A table consisting of the hubs in the maximum spanning tree is provided in Supplementary Table 5.

A summary of the frequencies at which the different centrality measures are significant in every analysis technique is provided in Table 3. The hubs commonly identified from the techniques mentioned above are represented in Fig. 8. A table consisting of the hubs commonly identified in all techniques mentioned above is provided in Table 4.

4. Discussion

The current study aims to investigate the differences in the functional network topology between tinnitus and healthy control subjects. The two hypothesized models of network topology are that (a) the tinnitus network could be a fundamentally different network when compared to the control network, i.e. have different hubs or (b) could be made up of the same nodes as the control network but connected differently. The first proposition is based on the theoretical model for the disease network in protein and genetic interactomes, which suggests that a functional disintegration of the normal genetic interactome leads to the formation of a distinct set of functional modules for different disorders (Barabási, 2007; Barabasi et al., 2011). There is also evidence from damage modeling studies in brain networks that suggest that there is disruption of the normal functional connectome leading to different functional networks in the presence of different disorders, in other words that many brain disorders are hub disorders of the hubs with highest centrality (Crossley et al., 2014; Kaiser et al., 2007). Also, tinnitus has been termed as a multi-modal disorder where the functional network is composed of individual, separable subnetworks that encode each behavioral symptom experienced by patients (De Ridder et al., 2014b) which creates the possibility of the tinnitus network consisting of functionally different hubs compared to a healthy control network. The second model is based on the changes in the different resting state networks observed in tinnitus (Schlee et al., 2009; Schmidt et al.,
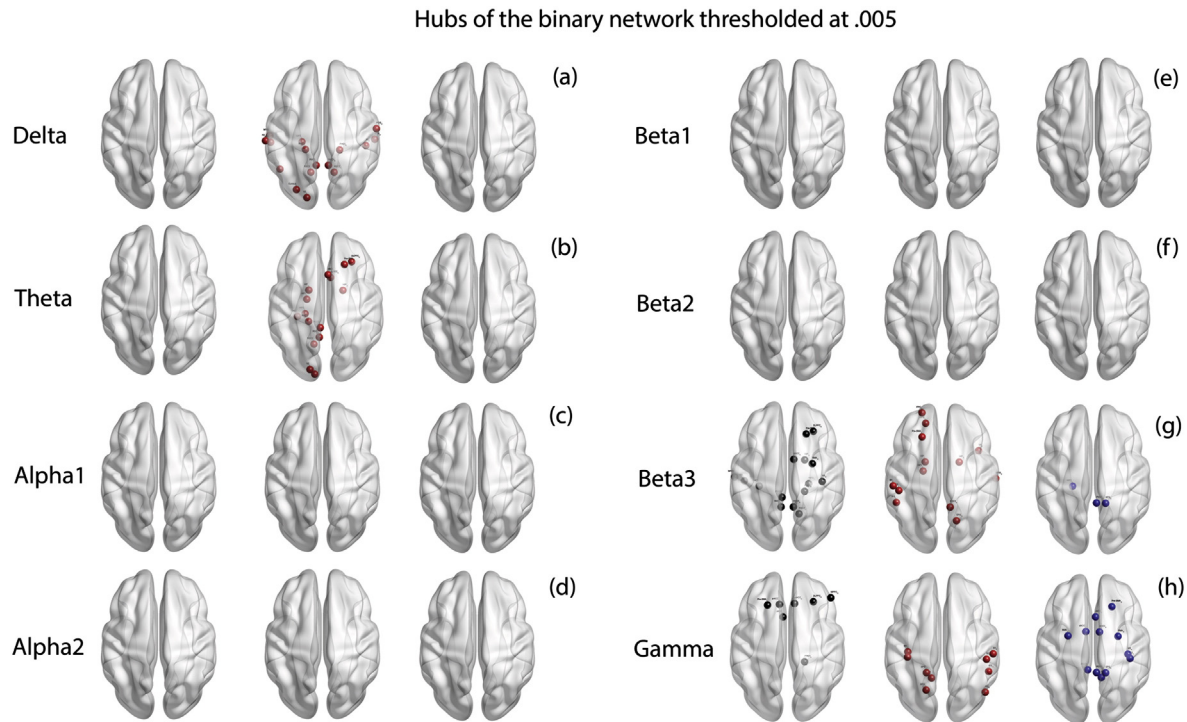
Hubs of the binary network thresholded at .005

Fig. 6. Hubs of the binary network thresholded at .005. (a)–(h) represent the hubs identified in the binary network thresholded at .005 in *left*: controls (black dots) only, *middle*: tinnitus (red dots) only and *right*: those hubs that are common to both tinnitus and control groups (blue dots) in (a) delta, (b) theta, (c) alpha1, (d) alpha2, (e) beta1, (f) beta2, (g) beta3 and (h) gamma frequency bands. (For interpretation of the references to color in this figure legend, the reader is referred to the web version of this article.)

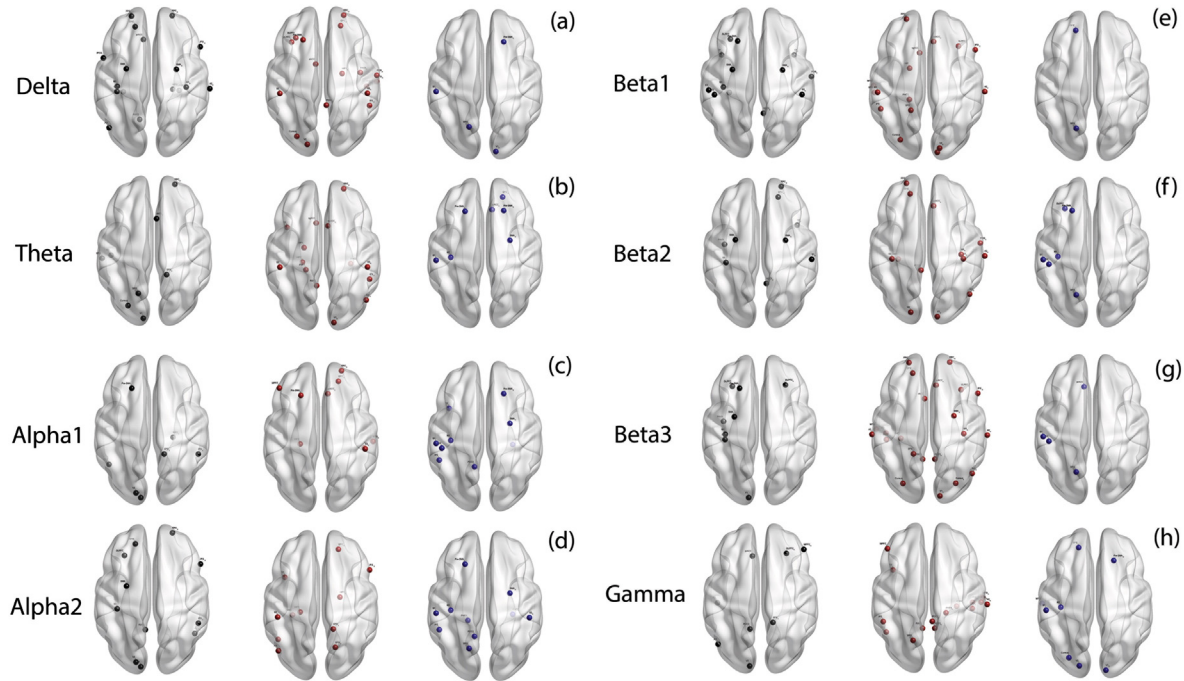## Hubs of the maximum spanning tree analysis

Fig. 7. Hubs of the maximum spanning tree. (a)–(h) represent the hubs identified in the by the maximum spanning tree in *left*: controls (black dots) only, *middle*: tinnitus (red dots) only and *right*: those hubs that are common to both tinnitus and control groups (blue dots) in (a) delta, (b) theta, (c) alpha1, (d) alpha2, (e) beta1, (f) beta2, (g) beta3 and (h) gamma frequency bands. (For interpretation of the references to color in this figure legend, the reader is referred to the web version of this article.)

2013) and the similarity in hubs between tinnitus (Husain and Schmidt, 2014; Schmidt et al., 2013) and other neuropathologies such as Parkinson's (Olde Dubbelink et al., 2014), Alzheimer's (Stam et al., 2007, 2009), schizophrenia (Bassett et al., 2008; Fornito and Bullmore, 2015), dementia (Agosta et al., 2013) and traumatic brain injury (Stam, 2014). This similarity combined with changes in resting state networks as observed by several imaging studies (Burton et al., 2012; Husain and Schmidt, 2014; Maudoux et al., 2012; Schmidt et al., 2013) encourage us to think that tinnitus is the result of rewiring hubs in existing functional networks.

In order to verify the above concept, different techniques were administered to identify the hubs of the tinnitus and control networks in order to cross-validate the results obtained from each of the techniques. Weighted matrices can produce results that are biased since those connections that have more weights are given more preference in the calculation of the centrality of the network. Hence, these were cross-validated with binary matrices. From the average node strength of the full network, we observe that the weights on the connections is different in different frequency bands even within the same group. In addition there exists a group difference for the node strength at each frequency band. Thus the differences in results between the weighted and binary networks while applying a constant threshold of .005 can be attributed to the difference in the number of edges in the tinnitus and control networks. To alleviate this problem, we used the maximum spanning tree analysis which compares two networks of equal number

of edges and nodes (Stam et al., 2014). However, this analysis only looks at the most important 83 connections of the network and neglects the other connections. Hence we constructed binary matrices with equal number of edges in the tinnitus and control network by introducing an appropriate threshold in each frequency band. The difference between the results from these binary matrices and the fully-connected weighted matrix can be attributed to the difference in the number of edges and the presence of weights.

Thus from the different analysis techniques, minimal overlap of hubs of the tinnitus and control networks would support hypothesis (a), a large overlap between the hubs of the two groups would support hypothesis (b) and a combination of overlap of hubs and change in network connectivity measures would indicate a combination of hypothesis (a) and (b). The results show that at the core, the tinnitus and control networks show a moderate overlap of hubs across all frequency bands. However, as the networks build up with more edges, we observe that the frequency bands influence the overlap of hubs between the two groups. The hubs in all the frequency bands, except the gamma frequency band, retain the minimum to moderate overlap between the hubs of the two groups. This effect is observed in both the binary and weighted networks and indicates that the difference between the tinnitus and control networks in all of the frequency bands except the gamma frequency band is probably driven by the modification of the hubs of the network. The modification of hubs is also accompanied by changes in network connectivity as characterized by changes in

Table 3

Oscillatory bands in which the simple contrast between tinnitus and control groups yield a significant difference for different network measures (betweenness centrality, node strength, eigenvector centrality and closeness centrality) calculated using different techniques.

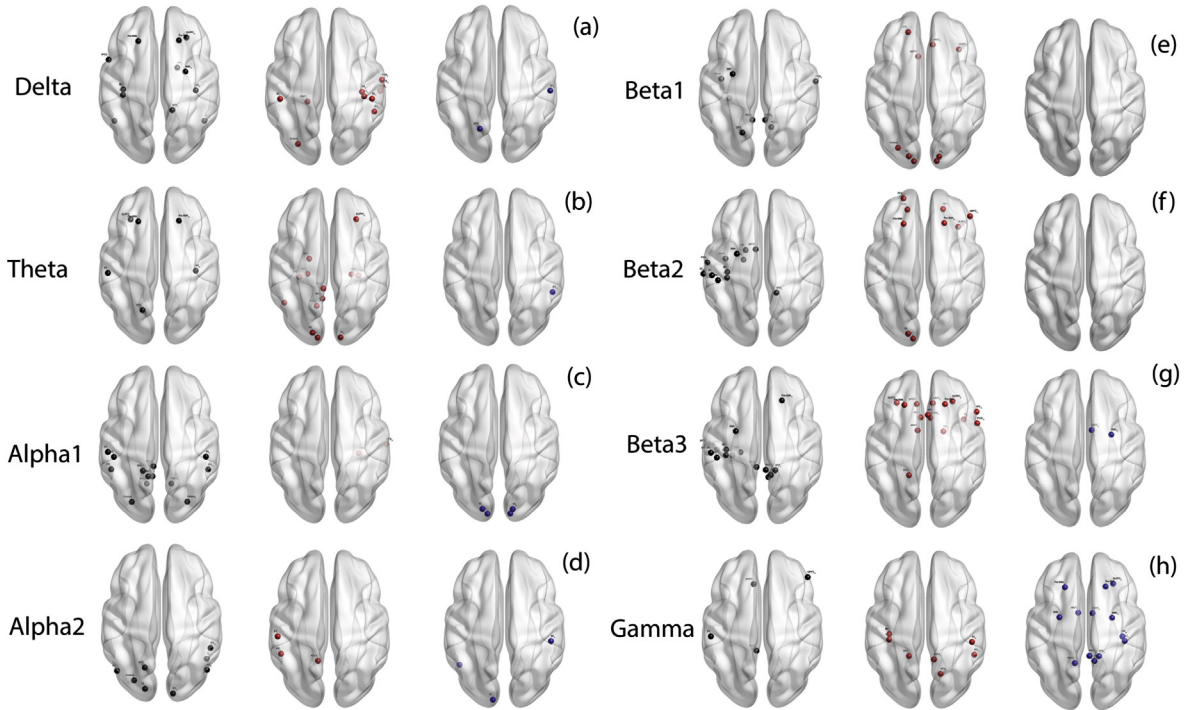| Network measure/technique	Betweenness centrality	Node strength	Eigenvector centrality	Closeness centrality
Fully-connected weighted network	–	δ, θ, α2, β1, β2, β3	–	δ, α1, α2, β1, β2, β3, γ
Fully-connected binary network with equal edges	–	θ, β1, β2, β3	–	δ, θ, β2, β3, γ
Weighted network thresholded at .005	δ, θ, α1, α2, β1, β2, γ	δ, θ, α2, β1, β2, β3, γ	β3, γ	δ, θ, α1, α2, β1, β2, β3, γ
Binary network thresholded at .005	δ, θ, α2, β1, β2, β3, γ	δ, θ, β2, β3, γ	–	δ, θ, β2, β3, γ
Maximum spanning tree	β3	–	–	–

Hubs common to all analysis techniques

Fig. 8. Hubs common to all analysis techniques. (a)–(h) represent the common hubs identified from all the techniques in *left*: controls (black dots) only, *middle*: tinnitus (red dots) only and *right*: those hubs that are common to both tinnitus and control groups (blue dots) in (a) delta, (b) theta, (c) alpha1, (d) alpha2, (e) beta1, (f) beta2, (g) beta3 and (h) gamma frequency bands. (For interpretation of the references to color in this figure legend, the reader is referred to the web version of this article.)

node strength and closeness centrality only in the delta, theta and beta3 frequency bands, and not in the alpha and lower beta bands. Thus, the difference in network topology in the delta, theta and beta3 bands is driven by changes in both hubs and network connectivity, whereas in the alpha and lower beta bands, the difference is driven only by changes in hubs. In our previous work we showed that the tinnitus network shifts to a more lattice topology in the lower frequencies and a random topology in the higher frequencies (Mohan et al., 2016). We observe that this change is more prevalent in the delta, theta and beta3 band

than in the alpha and lower beta bands. Changes in both hubs and connectivity offers more degrees of freedom and thus the shift in network topology possibly demands the higher degrees of freedom. In the gamma frequency band, we observe a significant overlap of hubs between the tinnitus and control groups. In addition, there is a significant difference in the node strength and closeness centrality measures between the tinnitus and control groups in both the binary and weighted networks indicating that the difference in the network topology between the two groups in the gamma frequency band is mostly driven

Table 4
Hubs that are common to all techniques.

Frequency band	Groups	Areas
Delta	Control	*Left*: S3, M1, pre-SMA, OTC, IPCG; *right*: SPS, pre-SMA, DLPFC, HIP, OTC, SMA, M1
	Tinnitus	*Left*: S2, cuneus, PCG, PHC1; *right*: S2, S3, M1, MTG, STG, IPS
	Common hubs	*Left*: SPG; *right*: S1
Theta	Control	*Left*: S1, SPG, pre-SMA, DLPFC; *right*: M1, pre-SMA
	Tinnitus	*Left*: V1, V2, HIP1, RSC1, RSC2, OTC, PCC1, HIP2, PHC2; *right*: DLPFC, V1, HIP2, PHC2
	Common hubs	*Right*: IPS
Alpha1	Control	*Left*: S1, S2, SPS, cuneus, PCC1, RSC1, RSC2, PCC2, IPS; *right*: S2, cuneus, RSC2, IPS
	Tinnitus	*Right*: MTG, PHC2
	Common hubs	*Left*: V1, V2; *right*: V1, V2
Alpha2	Control	*Left*: SPG, V2, cuneus, AG; *right*: V2, OTC, AG, IPS
	Tinnitus	*Left*: S1, PCC2, IPS
	Common hubs	*Left*: V1, V2; *right*: V1, V2
Beta1	Control	*Left*: SMA, SPG, insula, RSC1, PHC2; *right*: RSC1, RSC2, PCG
	Tinnitus	*Left*: OFC, V1, V2, cuneus, sgACC; *right*: V1, V2, prACC, VLPFC
	Common hubs	–
Beta2	Control	*Left*: S1, S2, S3, M1, SMA, insula, STG, dACC, HIP1, HIP, A2, PCG; *right*: SPS
	Tinnitus	*Left*: pre-SMA, FPC, OFC, V1, V2, ITG; *right*: pre-SMA, OFC, MPFC, VLPFC
	Common Hubs	–
Beta3	Control	*Left*: S1, S2, S3, M1, SMA, ITG, MTG, PCC1, PHC2, HIP2; *right*: SPS, PCC1, PCC2, RSC1, pre-SMA
	Tinnitus	*Left*: SPS, pre-SMA, DLPFC, dACC, prACC, rACC; right: pre-SMA, DLPFC, sgACC, prACC, rACC, HIP, TP, IPCG
	Common hubs	*Right*: dACC, SMA
Gamma	Control	*Left*: S1, PCC1, prACC; *right*: MPFC
	Tinnitus	*Left*: S3, M1, SPS; *right*: S2, SPG, PCC2, IPS
	Common hubs	*Left*: SMA, pre-SMA, PCC2, dACC; *right*: S3, M1, SPS, SMA, pre-SMA, DLPFC, PCC1, PCC2, dACC

by changes in network connectivity. In summary, the brain undergoes both changes in wiring pattern and wiring strength between different areas in tinnitus.

The frequency-specific reorganization of the brain in tinnitus can be attributed to the diverse hypotheses governing the tinnitus world. Among the different etiologies, sensory deafferentation is one of the most common and leading cause of tinnitus (Jastreboff, 1990; Noreña and Farley, 2013). The theory is that the lack of sensory input creates a disparity between the bottom-up sensory information and top-down prediction related to the sensory information thus producing a prediction error and sensory uncertainty (De Ridder et al., 2014a). This sensory uncertainty creates a top-down goal related direction towards the missing input (Fecteau and Munoz, 2006). The missing input is thus "filled in" as a solution to the Bayesian prediction error (De Ridder et al., 2014a) or if the sensory damage is severe, the missing input is pulled out from memory (De Ridder et al., 2011). Recent research shows that any sensation becomes a perception only when it is brought to the consciousness of the subject (Dehaene et al., 2006). Thus bringing the solution of the uncertainty, in other words tinnitus, to consciousness has been shown to involve the structures of the global workspace (Schlee et al., 2009). Although these different aspects of the theory are governed by different networks, they are integrated together by means of long-distance connections (von Stein and Sarnthein, 2000). The resulting tinnitus, as mentioned before is a multi-symptom disorder where patients experience different levels of loudness, distress and type of tinnitus which is encoded by different subnetworks. We observe that the different networks responsible for the different mechanisms of tinnitus production and maintenance can be identified in the different frequency bands in the current study.

Sensory deafferentation due to hearing loss or cochlear damage leads to salience of the bottom-up stimulus leading to top-down goal related direction towards the missing stimulus (Fecteau and Munoz, 2006). This salience is propagated using a feedback mechanism in the beta band (Arnal and Giraud, 2016) and is controlled primarily by the dorsal anterior cingulate cortex, anterior insula (Sadaghiani et al., 2009; van Marle et al., 2010), along with the pregenal anterior cingulate cortex and other deeper structures (Seeley et al., 2007). In the present study, we observe that the dorsal and the pregenual anterior cingulate cortices are the important hubs in the tinnitus group in the beta3 frequency band. This is consistent with the idea that tinnitus could be the result of a Bayesian prediction error or salience that is fed back by the dorsal and pregenual anterior cingulate cortices in the beta3 frequency band (De Ridder et al., 2014a). The dorsal, pregrnual and subgenual anterior cingulate cortex are also part of the distress network (Husain and Schmidt, 2014; Mayberg et al., 2005; Vanneste et al., 2010a; Weisz et al., 2005). Compensation of the deafferented input by "filling in the missing information" from memory has been reported to take place in the theta band (De Ridder et al., 2013; Vanneste et al., 2011c). We observe that the hubs in the theta band consist of the primary and secondary auditory cortices, frontal and parietal areas such as the dorsolateral pre-frontal cortex, superior parietal sulcus, inferior parietal sulcus and temporal areas such as the parahippocampal and hippocampal areas, retrosplenial cortices, superior, medial and inferior temporal gyri. The co-occurrence of the auditory cortices, parahippocampal and hippocampal areas and the dorsolateral prefrontal cortex in the tinnitus group in the theta band is consistent with the previous literature and could be further evidence to a possible subnetwork working to retrieve the deafferentiated sensory input from memory (De Ridder et al., 2006, 2011, 2014b).

Tinnitus, whether retrieved from memory (De Ridder et al., 2011) or a solution to the Bayesian prediction error (De Ridder et al., 2014a), has to be brought to consciousness for it to be perceived as a phantom sound. This is proposed to be related to parieto-frontal connections in the gamma band (Dehaene et al., 2006). In the gamma band we observe the presence of these parieto-frontal connections in both the tinnitus and control groups consisting of the superior parietal sulcus, inferior

parietal sulcus, the superior parietal gyrus and the dorsolateral prefrontal cortex. However, there is a significant increase in connectivity strength among these hubs in the tinnitus group compared to the control group and this finding is consistent with previous research (Schlee et al., 2009; Schmidt et al., 2013). These parieto-frontal areas constitute a fronto-parietal control network, linked to attention, both for goal directed and external stimuli (Corbetta and Shulman, 2002) as for memory related information (Cabeza et al., 2008).

Although salience, solution to the uncertainty and conscious perception of the tinnitus is proposed to be governed by different networks, functional integration of these processes is probably mediated by the lower frequencies, specifically the delta and the alpha bands (von Stein and Sarnthein, 2000). Alpha oscillations are associated with (a) updating Bayesian prediction errors (Arnal et al., 2014), (b) conscious awareness of stimuli (Palva and Palva, 2007) and (c) long-range cortical integration for meeting task requirements (von Stein and Sarnthein, 2000). From the current study, we observe that some of the hubs in the tinnitus and control group in the alpha frequency bands overlap, but some are unique to the tinnitus group. The hubs, such as precuneus, posterior cingulate cortex, angular gyrus as identified by imaging researchers to be a part of the default mode network (Mantini et al., 2007), are present in both the tinnitus and control groups which alludes to the involvement of the default mode network in tinnitus. This supports previous research (Husain and Schmidt, 2014; Schmidt et al., 2013). In addition, hubs involved in the long distance parieto-frontal connections and in the retrieval of tinnitus from memory are also observed in both the alpha bands only in the tinnitus group.

When looking at the overlapping hubs in the tinnitus brain and controls common to all techniques, it is obvious that the tinnitus brain and non-tinnitus brain differ dramatically in their topological structure. There are almost no overlapping hubs, suggesting that tinnitus is not the result of one phrenologically overactive area, but the emergent property of a completely changed brain topology. This could be related to the fact that tinnitus is not just a phantom sound perception, but is often associated with other clinical symptoms such as distress/anxiety, depression, cognitive deficiencies such as memory and concentration problems, etc. which are also associated with altered brain topology. Thus, this finding is compatible with a previously proposed model that suggests that the unified tinnitus percept is an emergent property of multiple parallel but interacting subnetworks (De Ridder et al., 2014b), which seems to be associated with a globally altered brain topological structure.

In short, the current research provides a good understanding of how the normal human connectome changes in the different frequency bands in association with the percept of phantom sound, as in tinnitus.

Although the results of the current study are promising in describing the differences in functional network topology in tinnitus and controls, there are some limitations of the study that have to be addressed. One of the major drawbacks of the study is the lack of an accurate control group that accounts for age, hearing loss and gender that have all shown to be confounding variables in tinnitus literature. The aim of the study was to look at fundamental differences in a group with and without tinnitus retrospectively so as to weigh the scope of the current procedure. Moving forward stricter conditions on the recruitment of subjects should be placed to cross-validate the results of the current study. Secondly, source-localization in an indirect way of estimating the activity at the source, due to the restricted spatial resolution of EEG. Thus, cross-validation of the results of the current study using techniques that more precisely estimate activity in brain regions should be done. Nevertheless, we see that fundamental differences lay between the organization of the functional networks between tinnitus and controls that encourage us to delve deeper into this venture.

5. Conclusion

The skeleton of the tinnitus network seems to be organized as a functional network different from the control network in all of the

frequency bands. However, when the network begins to build up more connections, the distinction between the network topology of tinnitus and control networks becomes frequency dependent. The overlap between the hubs of the tinnitus and control networks is maximum in the gamma frequency band and minimum in the delta, theta and beta bands. The overlap of hubs in the alpha bands is intermediate. Thus, the functional topology in gamma is analogous to a transformer model in which the difference between the tinnitus and control networks is mostly driven by changes in connectivity. The functional network in the other frequency bands is analogous to genetic networks in which there are distinct networks for control and disease conditions with some overlap among the hubs of the different networks. The modification of the hubs in the delta, theta and higher beta bands is also accompanied by changes in network connectivity. We can therefore conclude that the maladaptive tinnitus network undergoes changes in hubs as well as changes in connectivity, offering more degrees of freedom for the brain to change in order to compensate for the sensory deafferentation.

Conflict of interests

There are no conflicts of interest or competing financial interests among the authors.

Declaration of authorship

The contributions of the authors are as follows:

AM: data analysis, writing paper; DDR: collecting data, writing paper; SV: collecting data, data analysis and writing paper.

There is no conflict among the authors in deciding authorship on the paper.

Declaration of submission

All the authors on the paper declare that the paper has not been published elsewhere.

Appendix A. Supplementary data

Supplementary data to this article can be found online at http://dx.doi.org/10.1016/j.nicl.2016.01.022.

References

Achard, S., Bullmore, E., 2007. Efficiency and cost of economical brain functional networks. PLoS Comput. Biol. 3, e17.

Agosta, F., Sala, S., Valsasina, P., Meani, A., Canu, E., Magnani, G., Cappa, S.F., Scola, E., Quatto, P., Horsfield, M.A., Falini, A., Comi, G., Filippi, M., 2013. Brain network connectivity assessed using graph theory in frontotemporal dementia. Neurology. 81(2), 134–143.

Albert, R., Barabási, A.-L., 2002. Statistical mechanics of complex networks. Rev. Mod. Phys. 74, 47–97.

Arnal, L.H., Giraud, A.-L., 2016. Cortical oscillations and sensory predictions. Trends Cogn. Sci. 16, 390–398.

Arnal, L.H., Doelling, K.B., Poeppel, D., 2014. Delta–Beta Coupled Oscillations Underlie Temporal Prediction Accuracy Cereb Cortex.

Audiology, B.S.o., 2008. Recommended Procedure: Pure Tone Air and Bone Conduction Threshold Audiometry With and Without Masking and Determination of Uncomfortable Loudness Levels.

Barabási, A.-L., 2007. Network medicine — from obesity to the "diseasome". N. Engl. J. Med. 357, 404–407.

Barabasi, A.L., Albert, R., 1999. Emergence of scaling in random networks. Science 286, 509–512.

Barabasi, A.-L., Gulbahce, N., Loscalzo, J., 2011. Network medicine: a network-based approach to human disease. Nat. Rev. Genet. 12, 56–68.

Bassett, D.S., Bullmore, E., 2006. Small-world brain networks. Neuroscientist 12, 512–523.

Bassett, D.S., Bullmore, E., Verchinski, B.A., Mattay, V.S., Weinberger, D.R., Meyer-Lindenberg, A., 2008. Hierarchical organization of human cortical networks in health and schizophrenia. J. Neurosci. 28, 9239–9248.

Bullmore, E., Sporns, O., 2009. Complex brain networks: graph theoretical analysis of structural and functional systems. Nat. Rev. Neurosci. 10, 186–198.

Bullmore, E., Sporns, O., 2012. The economy of brain network organization. Nat. Rev. Neurosci. 13, 336–349.

Burton, H., Wineland, A., Bhattacharya, M., Nicklaus, J., Garcia, K., Piccirillo, J., 2012. Altered networks in bothersome tinnitus: a functional connectivity study. BMC Neurosci. 13, 3.

Cabeza, R., Ciaramelli, E., Olson, I.R., Moscovitch, M., 2008. The parietal cortex and episodic memory: an attentional account. Nat. Rev. Neurosci. 9, 613–625.

Congedo, M., 2002. EureKa! (Version 3.0) [Computer Software]. NovaTech EEG Inc., Knoxville, TN (Freeware available at www.NovaTechEEG).

Congedo, M., John, R.E., De Ridder, D., Prichep, L., Isenhart, R., 2010. On the "dependence" of "independent" group EEG sources; an EEG study on two large databases. Brain Topogr. 23, 134–138.

Corbetta, M., Shulman, G.L., 2002. Control of goal-directed and stimulus-driven attention in the brain. Nat. Rev. Neurosci. 3, 201–215.

Crossley, N.A., Mechelli, A., Scott, J., Carletti, F., Fox, P.T., McGuire, P., Bullmore, E.T., 2014. The hubs of the human connectome are generally implicated in the anatomy of brain disorders. Brain 137, 2382–2395.

De Ridder, D., Fransen, H., Francois, O., Sunaert, S., Kovacs, S., Van De Heyning, P., 2006. Amygdalohippocampal involvement in tinnitus and auditory memory. Acta Otolaryngol. Suppl. 50-53.

De Ridder, D., Elgoyhen, A.B., Romo, R., Langguth, B., 2011. Phantom percepts: tinnitus and pain as persisting aversive memory networks. Proc. Natl. Acad. Sci. 108, 8075–8080.

De Ridder, D., Song, J.-J., Vanneste, S., 2013. Frontal cortex TMS for tinnitus. Brain Stimul. 6, 355–362.

De Ridder, D., Vanneste, S., Freeman, W., 2014a. The Bayesian brain: phantom percepts resolve sensory uncertainty. Neurosci. Biobehav. Rev. 44, 4–15.

De Ridder, D., Vanneste, S., Weisz, N., Londero, A., Schlee, W., Elgoyhen, A.B., Langguth, B., 2014b. An integrative model of auditory phantom perception: tinnitus as a unified percept of interacting separable subnetworks. Neurosci. Biobehav. Rev. 44, 16–32.

Dehaene, S., Changeux, J.-P., Naccache, L., Sackur, J., Sergent, C., 2006. Conscious, preconscious, and subliminal processing: a testable taxonomy. Trends Cogn. Sci. 10, 204–211.

Dijkstra, E.W., 1959. A note on two problems in connexion with graphs. Numer. Math. 1, 269–271.

Fecteau, J.H., Munoz, D.P., 2006. Salience, relevance, and firing: a priority map for target selection. Trends Cogn. Sci. 10, 382–390.

Fornito, A., Bullmore, E.T., 2015. Reconciling abnormalities of brain network structure and function in schizophrenia. Curr. Opin. Neurobiol. 30, 44–50.

Hartmann, T., Lorenz, I., Müller, N., Langguth, B., Weisz, N., 2014. The effects of neurofeedback on oscillatory processes related to tinnitus. Brain Topogr. 27, 149–157.

Husain, F.T., Schmidt, S.A., 2014. Using resting state functional connectivity to unravel networks of tinnitus. Hear. Res. 307, 153–162.

Jastreboff, P.J., 1990. Phantom auditory perception (tinnitus): mechanisms of generation and perception. Neurosci. Res. 8, 221–254.

Kaiser, M., Varier, S., 2011. Evolution and development of brain networks: from Caenorhabditis elegans to Homo sapiens. Netw. Comput. Neural Syst. 22, 143–147.

Kaiser, M., Martin, R., Andras, P., Young, M.P., 2007. Simulation of robustness against lesions of cortical networks. Eur. J. Neurosci. 25, 3185–3192.

Kruskal Jr., J.B., 1956. On the shortest spanning subtree of a graph and the traveling salesman problem. Proc. Am. Math. Soc. 7, 48–50.

Langer, N., Pedroni, A., Jäncke, L., 2013. The problem of thresholding in small-world network analysis. PLoS One 8, e53199.

Lanting, C.P., de Kleine, E., Langers, D.R.M., van Dijk, P., 2014. Unilateral tinnitus: changes in connectivity and response lateralization measured with fMRI. PLoS One 9, e110704.

Latora, V., Marchiori, M., 2003. Economic small-world behavior in weighted networks. Eur. Phys. J. B 32, 249–263.

Laureano, M.R., Onishi, E.T., Bressan, R.A., Castiglioni, M.L.V., Batista, I.R., Reis, M.A., Garcia, M.V., de Andrade, A.N., de Almeida, R.R., Garrido, G.J., Jackowski, A.P., 2014. Memory networks in tinnitus: a functional brain image study. PLoS One 9, e87839.

Mantini, D., Perrucci, M.G., Del Gratta, C., Romani, G.L., Corbetta, M., 2007. Electrophysiological signatures of resting state networks in the human brain. Proc. Natl. Acad. Sci. U. S. A. 104, 13170–13175.

Maslov, S., Sneppen, K., 2002. Specificity and stability in topology of protein networks. Science 296, 910–913.

Maudoux, A., Lefebvre, P., Cabay, J.-E., Demertzi, A., Vanhaudenhuyse, A., Laureys, S., Soddu, A., 2012. Auditory resting-state network connectivity in tinnitus: a functional MRI study. PLoS One 7, e36222.

Mayberg, H.S., Lozano, A.M., Voon, V., McNeely, H.E., Seminowicz, D., Hamani, C., Schwalb, J.M., Kennedy, S.H., 2005. Deep brain stimulation for treatment-resistant depression. Neuron 45, 651–660.

Meeus, O., Heyndrickx, K., Lambrechts, P., De Ridder, D., Van de Heyning, P., 2009. Phaseshift treatment for tinnitus of cochlear origin. Eur. Arch. Otorhinolaryngol.

Meeus, O., De Ridder, D., Van de Heyning, P., 2011. Administration of the Combination Clonazepam–Deanxit as Treatment for Tinnitus Otol Neurotol.

Mohan, A., De Ridder, D., Vanneste, S., 2016. Graph theoretical analysis of brain connectivity in phantom sound perception. Sci. Rep. 6, 19683 http://www.nature.com/articles/srep19683.

Noreña, A.J., Farley, B.J., 2013. Tinnitus-related neural activity: theories of generation, propagation, and centralization. Hear. Res. 295, 161–171.

Olde Dubbelink, K.T.E., Hillebrand, A., Stoffers, D., Deijen, J.B., Twisk, J.W.R., Stam, C.J., Berendse, H.W., 2014. Disrupted brain network topology in Parkinson's disease: a longitudinal magnetoencephalography study.

Palva, S., Palva, J.M., 2007. New vistas for α-frequency band oscillations. Trends Neurosci. 30, 150–158.

Pascual-Marqui, R.D., 2002. Standardized low-resolution brain electromagnetic tomography (sLORETA): technical details. Methods Find. Exp. Clin. Pharmacol. 24 (Suppl D), 5–12.

Pascual-Marqui, R.D., Lehmann, D., Koukkou, M., Kochi, K., Anderer, P., Saletu, B., Tanaka, H., Hirata, K., John, E.R., Prichep, L., Biscay-Lirio, R., Kinoshita, T., 2011. Assessing interactions in the brain with exact low-resolution electromagnetic tomography. Philos. Trans. R. Soc. Lond. A 369, 3768–3784.

Rubinov, M., Sporns, O., 2010. Complex network measures of brain connectivity: uses and interpretations. NeuroImage 52, 1059–1069.

Sadaghiani, S., Hesselmann, G., Kleinschmidt, A., 2009. Distributed and antagonistic contributions of ongoing activity fluctuations to auditory stimulus detection. J. Neurosci. 29, 13410–13417.

Schlee, W., Weisz, N., Dohrmann, K., Hartmann, T., Elbert, T., 2007. Unravelling the tinnitus distress network using single trial auditory steady-state responses. Int. Congr. Ser. 1300, 73–76.

Schlee, W., Mueller, N., Hartmann, T., Keil, J., Lorenz, I., Weisz, N., 2009. Mapping cortical hubs in tinnitus. BMC Biol. 7, 80-80.

Schmidt, S.A., Akrofi, K., Carpenter-Thompson, J.R., Husain, F.T., 2013. Default mode, dorsal attention and auditory resting state networks exhibit differential functional connectivity in tinnitus and hearing loss. PLoS One 8, e76488.

Seeley, W.W., Menon, V., Schatzberg, A.F., Keller, J., Glover, G.H., Kenna, H., Reiss, A.L., Greicius, M.D., 2007. Dissociable intrinsic connectivity networks for salience processing and executive control. J. Neurosci. 27, 2349–2356.

Song, J.J., De Ridder, D., Schlee, W., Van de Heyning, P., Vanneste, S., 2013a. "Distressed aging": the differences in brain activity between early- and late-onset tinnitus. Neurobiol. Aging.

Song, J.J., Punte, A.K., De Ridder, D., Vanneste, S., Van de Heyning, P., 2013b. Neural substrates predicting improvement of tinnitus after cochlear implantation in patients with single-sided deafness. Hear. Res. 299C, 1–9.

Sporns, O., Zwi, J.D., 2004. The small world of the cerebral cortex. Neuroinformatics 2, 145–162.

Stam, C.J., 2014. Modern network science of neurological disorders. Nat. Rev. Neurosci. 15, 683–695.

Stam, C.J., Jones, B.F., Nolte, G., Breakspear, M., Scheltens, P., 2007. Small-world networks and functional connectivity in Alzheimer's disease. Cereb. Cortex 17, 92–99.

Stam, C.J., de Haan, W., Daffertshofer, A., Jones, B.F., Manshanden, I., van Cappellen van Walsum, A.M., Montez, T., Verbunt, J.P., de Munck, J.C., van Dijk, B.W., Berendse, H.W., Scheltens, P., 2009. Graph theoretical analysis of magnetoencephalographic functional connectivity in Alzheimer's disease. Brain 132, 213–224.

Stam, C.J., Tewarie, P., Van Dellen, E., van Straaten, E.C.W., Hillebrand, A., Van Mieghem, P., 2014. The trees and the forest: characterization of complex brain networks with minimum spanning trees. Int. J. Psychophysiol. 92, 129–138.

Strogatz, S.H., 2001. Exploring complex networks. Nature 410, 268–276.

van den Heuvel, M.P., Sporns, O., 2011. Rich-club organization of the human connectome. J. Neurosci. 31, 15775–15786.

van Marle, H.J.F., Hermans, E.J., Qin, S., Fernández, G., 2010. Enhanced resting-state connectivity of amygdala in the immediate aftermath of acute psychological stress. NeuroImage 53, 348–354.

Vanneste, S., De Ridder, D., 2011. The use of alcohol as a moderator for tinnitus-related distress. Brain Topogr.

Vanneste, S., Plazier, M., Van Der Loo, E., Ost, J., Van de Heyning, P., De Ridder, D., 2010a. Burst transcranial magnetic stimulation: which tinnitus characteristics influence the amount of transient tinnitus suppression? Eur. J. Neurol. 17, 1141–1147.

Vanneste, S., Plazier, M., van der Loo, E., Van de Heyning, P., De Ridder, D., 2010b. The differences in brain activity between narrow band noise and pure tone tinnitus. PLoS One 5, e13618.

Vanneste, S., Plazier, M., van der Loo, E., Van de Heyning, P., De Ridder, D., 2011a. The difference between uni- and bilateral auditory phantom percept. Clin. Neurophysiol. 122, 578–587.

Vanneste, S., Van de Heyning, P., De Ridder, D., 2011b. Contralateral parahippocampal gamma-band activity determines noise-like tinnitus laterality: a region of interest analysis. Neuroscience 199, 481–490.

Vanneste, S., van de Heyning, P., De Ridder, D., 2011c. The neural network of phantom sound changes over time: a comparison between recent-onset and chronic tinnitus patients. Eur. J. Neurosci. 34, 718–731.

von Stein, A., Sarnthein, J., 2000. Different frequencies for different scales of cortical integration: from local gamma to long range alpha/theta synchronization. Int. J. Psychophysiol. 38, 301–313.

Wang, H., Douw, L., Hernández, J.M., Reijneveld, J.C., Stam, C.J., Van Mieghem, P., 2010. Effect of tumor resection on the characteristics of functional brain networks. Phys. Rev. E 82, 021924.

Watts, D.J., 1999. Networks, dynamics, and the small-world phenomenon. Am. J. Sociol. 105, 493–527.

Watts, D.J., Strogatz, S.H., 1998. Collective dynamics of 'small-world' networks. Nature 393, 440–442.

Weisz, N., Moratti, S., Meinzer, M., Dohrmann, K., Elbert, T., 2005. Tinnitus perception and distress is related to abnormal spontaneous brain activity as measured by magnetoencephalography. PLoS Med. 2, e153.

Zamora-López, G., Zhou, C., Kurths, J., 2010. Cortical hubs form a module for multisensory integration on top of the hierarchy of cortical networks. Front. Neuroinf. 4, 1.